Available online at www.sciencedirect.com
SCIENCE DIRECT
ELSEVIER
Nuclear Instruments and Methods in Physics Research A 546 (2005) 376–384
NUCLEAR INSTRUMENTS & METHODS IN PHYSICS RESEARCH Section A
www.elsevier.com/locate/nima

A photon beam polarimeter based on nuclear e^+e^- pair production in an amorphous target

F. Adamyan[a], H. Hakobyan[a], R. Jones[b], Zh. Manukyan[a], A. Sirunyan[a,*], H. Vartapetian[a]

[a] *Yerevan Physics Institute, 2 Alikhanian Brother str., EPD, 375036, Yerevan, Armenia*
[b] *University of Connecticut, Storrs, CT, USA*

Received 3 February 2005; accepted 15 February 2005
Available online 27 April 2005

Abstract

To directly measure the linear polarization of coherent bremsstrahlung (CB) photons with a peak energy of 1 GeV at the Yerevan synchrotron, a simple polarimeter is proposed based on a e^+e^- pair spectrometer equipped with two hodoscopes of scintillating counters positioned above and below of the median plane, configured to detect symmetric pairs produced in an amorphous target. Monte Carlo calculations show that the use of a vertical slit collimator at the entrance of the magnet improves both the analyzing power and the energy resolution. The values of the analyzing power for various atomic form factors of the target (the 20 μm of aluminum) reach a 0.25–0.28 with expected yields of useful events on the level of a few Hz at nominal operating intensity.

PACS: 14.70.Bh; 24.70.+s; 78.70.−g

Keywords: Analyzing power; Polarimeter; Linear polarization; Bremsstrahlung

1. Introduction

Linearly polarized coherent bremsstrahlung (CB) photon beams are widely used in the study of photonuclear reactions. To carry out experiments with CB beams, it is necessary to know the polarization with high accuracy. In an ideal experiment, the photon beam linear polarization can be calculated based upon the theoretical description of the CB process [1–3]. One established technique is to incorporate a number of known experimental factors into the theoretical model as free parameters, and then determine their values by comparing the theoretical and measured

*Corresponding author. Tel.: +3741 342747; fax: +3741 398392.
E-mail address: sirunian@mail.yerphi.am (A. Sirunyan).

0168-9002/$ - see front matter © 2005 Elsevier B.V. All rights reserved.
doi:10.1016/j.nima.2005.02.037

intensity spectra [4–6]. Thus calibrated the theoretical model is then used to predict the beam polarization.

Direct methods for photon polarimetry in the 1–10 GeV range include incoherent e^+e^- pair production in an amorphous target [7–10], pair production in an oriental crystal [1,2], and triplet production [11]. Of the three methods, the first is the most efficient in terms of the simplicity of the experimental setup and sensitivity to systematic effects. This technique involves measuring the azimuthal distribution about the beam axis of e^+e^- pairs produced in a thin amorphous target. Applications of this technique in early experiments carried out so far [7–10], exploited an asymmetrical detector acceptance for the e^+e^- pairs, where the kinematics of the e^+ were selected (E_+, θ_+, φ_+) and the remaining kinematic variables (E_-, θ_-) were integrated out, leading to a relatively low analyzing power of approximately 10%. A general survey of the differential cross-section, analyzing power and figure of merit for incoherent pair production is given in Ref. [12]. Based on their analysis, which covered electron and positron production angles up to $1.5\,\mathrm{m}/E$, the authors recommended a detector configuration that selects non-coplanar pairs, leading to a high analyzing power but rather low figure of merit. Ref. [13] presents a concrete design for a polarimeter following the approach of Ref. [12], based upon a thin amorphous target, silicon microstrip detectors for measuring the azimuthal angles of the two tracks, and a dipole pair spectrometer for energy analysis. Ref. [14] proposed an alternate set of detection kinematics, with $E_+ = E_-$, $\theta_+ = \theta_-$, $\varphi_+ = \varphi_-$. These so-called "wedge and ring" kinematics lead to an analyzing power of 30%, as derived from numerical calculations based upon the formalism presented in Ref. [9].

The aim of the present paper is to describe the pair polarimeter that has been designed for the 1 GeV CB photon beam line at the Yerevan synchrotron. Monte Carlo studies of the polarimeter performance are presented, together with a method for calculating the expected polarization by exploiting the photon spectrum measured with a multichannel pair spectrometer.

2. Method of incoherent pair production

In Ref. [7] it was proposed for the first time that the process $Z(\gamma, e^+e^-)$ in an amorphous target be used to measure the linear polarization of a photon beam. The azimuthal asymmetry of e^+e^- pairs with momenta $\mathbf{P}_{e^+}$ and $\mathbf{P}_{e^-}$, polar angles θ_+, θ_- and azimuthal angles φ_+, φ_- is used to analyze polarization of a photon with 4 momentum $k(\mathbf{k}, E_\gamma)$ and polarization vector $\mathbf{P}$, as shown in Fig. 1. This method exploits the angular correlation between the photon beam polarization plane, which contains the vectors $\mathbf{P}$ and $\mathbf{k}$, and the production plane of the electron or positron, which contains the vectors $\mathbf{P}_+$ and k (or $\mathbf{P}_-$ and k). The azimuthal asymmetry, or analyzing power, of a particular experimental arrangement is defined as

$$A = \frac{\sigma_\parallel - \sigma_\perp}{\sigma_\parallel + \sigma_\perp} \tag{1}$$

where σ represents the cross-section for production of pair that falls within the detector acceptance: $\sigma_\parallel$ for an incident photon in the favored polarization state for the given setup, and $\sigma_\perp$ for the orthogonal polarization. This ratio has a large value when $\varphi_- - \varphi_+ \sim \pi$ (coplanar pairs). Maximon and Olsen [9] showed that it is possible to reach large values of the analyzing power by selecting e^+e^- pairs over a narrow range $\Delta\phi$ around the copolar direction (nearly coplanar pairs).

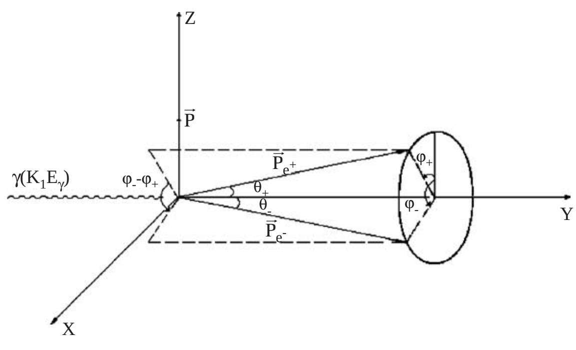

Fig. 1. Kinematics of the process $Z(\gamma, e^+e^-)$.

The analyzing power strongly depends on the experimental geometry. As is shown in Ref. [14] a high analyzing power may be obtained if symmetric e^+e^- pairs are selected, in combination with narrow angular ranges in both $\Delta\phi$ and $\Delta\theta$. Using this approach, we have developed a polarimeter design, based upon a magnetic spectrometer, which has an analyzing power as 0.3 in the vicinity of 1 GeV photon energy.

To calculate the pair production rate for linearly polarized photons in an amorphous target, we used the analytical expression for differential cross-section from Ref. [14] which depends on the target material through the atomic form factor $F(q)$:

$$\mathrm{d}^5\sigma = \frac{\sigma_0}{\pi^2} y(1-y) \frac{[1-F(q)]^2}{q^4} \times (X_{\mathrm{unp}} - \xi_3 X_{\mathrm{pol}})\,\mathrm{d}y\mathrm{d}u_-^2\mathrm{d}u_+^2\mathrm{d}\varphi_-\mathrm{d}\varphi_+ \tag{2}$$

where $\sigma_0 = Z^2 r^2 \alpha$, Z is the nuclear charge, r is the classical electron radius, $\alpha = 1/137$, $y = E_\pm/E_\gamma$, $u_\pm = E_\pm\theta_\pm/m$, ξ_3 is the Stokes parameter indicating whether the polarization vector **P** is parallel (+) or perpendicular (−) to the z-axis (see Fig. 1), and the remaining quantities are defined below.

$$q^2 = \frac{\delta^2}{m^2}[1+(1-y)u_+^2 + yu_-^2]^2 + u_+^2 + u_-^2 + 2u_+u_-\cos(\varphi_+ - \varphi_-) \tag{3}$$

$$X_{\mathrm{unp}} = (\xi_+ - \xi_-)^2 + \tfrac{1}{2}\varphi(y)\xi_+\xi_-[u_+^2 + u_-^2 + 2u_+u_-\cos(\varphi_+ - \varphi_-)] \tag{4}$$

$$X_{\mathrm{pol}} = \xi_+^2 u_+^2 \cos 2\varphi_+ + \xi_-^2 u_-^2 \cos 2\varphi_- + 2\xi_+\xi_- u_+u_-\cos(\varphi_+ + \varphi_-) \tag{5}$$

where q^2 is the square of momentum transfer in units of the electron mass squared, $\varphi(y) = y/(1-y) + (1-y)/y$, $\xi_\pm = 1/(1+u_\pm^2)$, and $\delta = m^2/2E_\gamma y(1-y)$ is the minimum momentum transfer for a given value of y. To investigate the influence of various atomic form factors on the pair production cross-section, we studied two choices for the atomic form factor $F(q)$,

$$F(q) = 1/[1+(111qZ^{-1/3})^2] \tag{6}$$

for the case of complete screening [9] and the Cromer-Waber (CW) form

$$F(q) = \frac{1}{Z}\left(\sum_{i=1}^{4} a_i e^{-b_i q^2} + c\right) \tag{7}$$

with parameters from Ref. [15].

The CW form is expected to give a more accurate parameterization of the atomic form factor [19], while a comparison with the standard dipole formula provides a means for estimating sensitivities.

The differential cross-section in terms of the dimensionless kinematic variables given in Eq. (2) can be expressed in terms of particle energy and angles in the laboratory frame using Eq. (8)

$$\frac{\mathrm{d}^5\sigma}{\mathrm{d}y\mathrm{d}u_-^2\mathrm{d}u_+^2\mathrm{d}\varphi_+\mathrm{d}\varphi_-} = \frac{E_\gamma m^4}{4E_+^2E_-^2}\frac{\mathrm{d}^5\sigma}{\mathrm{d}E_+\mathrm{d}\Omega_+\mathrm{d}\Omega_-}. \tag{8}$$

3. Yerevan synchrotron experimental conditions

At the beginning of the 1970's a linearly polarized photon beam was first obtained at the Yerevan synchrotron [16] and many polarization experiments were carried out. To determine the photon beam polarization several calculational methods were used based on the measured CB intensity spectrum [17,18]. With these methods, systematic errors on the calculated polarization P_γ were estimated to be at the level of 0.01 in the region of the CB peak, given by $\Delta E_\gamma/E_\gamma^{\mathrm{peak}} = 15$–$20\%$. A dominant factor in the systematic error on the calculated polarization came from the choice of atomic form factor, with different choices producing a band of width 0.02 in P_γ, within this energy range [19].

The present work proposes a direct measurement which can check the accuracy of the calculational approach, which is essential if these methods are to relied upon for future measurements. In doing so, it provides a means to determine the correct atomic form factor that applies to the CB process, as well as a check for the presence of other unanticipated sources of systematic errors.

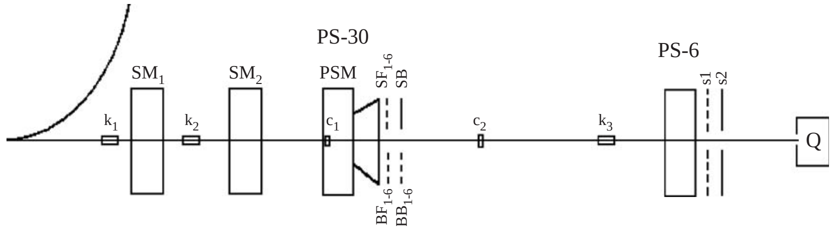

Fig. 2. Scheme of the experimental setup.

The photon beam linear polarization P_γ is related to a measured asymmetry by

$$P_\gamma = A^{\text{exp}}/A^{\text{cal}} \tag{9}$$

where A^{exp} is the experimental asymmetry on some observable in e^+e^- pair production, which depends implicitly on the form factor of the target atoms. A^{cal} is determined by Monte Carlo simulations of the experimental setup, based on the differential cross-section given in Eq. (2) for pair production from polarized photons with $P_\gamma = 1$, and an assumed form for the target form factor $F(q)$ [12,13,15].

A^{exp} is operationally defined as

$$A^{\text{exp}} = (N_1 - N_2)/(N_1 + N_2) \tag{10}$$

where N_1 and N_2 are the number of e^+e^- pairs produced by the linearly polarized photon beam (energy E_γ) for the two orthogonal orientations of the polarization vector. The experimental conditions are arranged to keep the value of P_γ the same for the two polarization settings of the beam.

Under these conditions the uncertainties of the experimental measurement of the photon beam linear polarization P_γ consist of the statistical uncertainties on the measured value of A^{exp} and the Monte Carlo estimate for A^{cal}, and systematic uncertainties associated with errors on the spectrometer energy calibration and alignment errors between the beam and acceptance-defining elements of the polarimeter. The sensitivity of A^{cal} to the experimental parameters is studied using Monte Carlo simulations.

A diagram of the CB beam line at the Yerevan synchrotron, as configured for the polarimetry measurement, is shown in Fig. 2. The CB photon beam enters the figure from the left, and passes through a pair of collimators, K_1 and K_2, which limit the angular divergence of the beam to a half-angle of 0.170 mr. Sweeping magnets SM_1 and SM_2 remove from the beam any charged particles created by beam interactions in the collimators. The collimated beam then passes through a thin converter C_1, made of 10 μm of lavsan polyethylene film. Pairs created in C_1 are analyzed and detected in the 30-channel pair spectrometer PS-30, which provides a continuous monitor of the photon beam intensity spectrum during the polarization measurement. The majority of the photon beam passes through converter C_1 without interaction and reaches a second converter target C_2, comprised of a 20 μm aluminum foil. Pairs created in C_2 pass through the acceptance-defining slit K_3, which provides the azimuthal selection required for polarimetry. Downstream of K_3 is a second pair spectrometer PS-6 (Fig. 3) which is equipped with counters above and below the median plane which record coincidences between electron and positron tracks. The entire path traversed by the beam and the detected pairs is inside vacuum up to the respective detector planes.

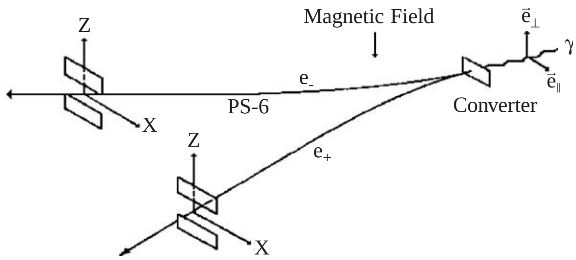

Fig. 3. Sketch of the polarimeter PS-6.

The magnetic field of PS-30 effectively removes from the beam any charged component produced upstream of C_2, so that the PS-6 detectors see only pairs produced in C_2.

For controlling systematic errors during the polarization measurement, it is necessary to record simultaneously beam spectra in the PS-30 and the PS-6 pair spectrometers. Under conditions of correct alignment, the intensity spectra in the two spectrometers should be in agreement. To achieve this, it is required that the relative placement of the collimator and polarimeter assembly be controlled with accuracy not worse than 1 mm in the coordinates transverse to the beam axis. In the energy range $E_\gamma = 900$–1100 MeV, the accuracy of the polarization measurement with this setup is expected to be 0.02.

This instrumentation provides the capacity for two independent determinations of the beam polarization. The photon intensity spectrum measured in the PS-30 spectrometer (1.5–2.0% energy resolution [20]) can be fitted to the expected CB intensity spectrum, superimposed upon a background of incoherent bremsstrahlung and folded with a generic resolution function which takes into account such effects as beam emittance, energy spread, and diamond imperfections [19]. The same model can then be used to predict the polarization spectral function, including all of the same experimental resolution effects, assuming some choice of atomic form factor $F(q)$. In principle, the intensity spectra also depend upon the atomic form factor, but that dependence is difficult to isolate in the presence of the resolution effects mentioned above. By contrast, the polarization asymmetry involves only ratios of intensities, leading in that case to the cancellation of many resolution effects.

Simultaneously with the indirect method based on data from the PS-30 spectrometer, the PS-6 spectrometer provides data for a direct determination of P_γ. The PS-6 detector array is divided into sections which lie above and below the median plane of the spectrometer, so that only pairs with significant transverse momentum with respect to the beam axis are detected. The presence of the vertical slit K_3 upstream of the PS-6 detector plane means that only pairs produced within a limited azimuthal range around the vertical are seen in the spectrometer. The slits of nominal aperture 2 cm are located 15.8 m downstream of the converter C_2, with the PS-6 detector plane located at 19.9 m. The polarization asymmetry is measured by alternating the plane of polarization at the source between the horizontal and vertical directions, and recording the changes in the coincidence rates in PS-6. Simultaneous monitoring of the intensity spectra in PS-30 ensure that the beam properties other than polarization are constant during the measurement. Comparison between measured and calculated polarization spectra allow the extraction of a measured atomic form factor over the range in q^2 that is accessible with the Yerevan CB source [21].

4. Monte Carlo simulations

In order to optimize the polarimeter geometry, including the sizes of hodoscopes counters and the aperture of collimator K_3, Monte Carlo calculations of luminosity, energy resolution and analyzing power were carried out. The calculations took into account all experimental conditions that were thought to be relevant, including the shape of CB spectrum, the size and divergence of the beam in the converters, multiple scattering and the magnetic field map of the PS-6 dipole. Simulation of e^+e^- pair production was carried out using the analytical expression for the differential cross-section given by Eq. (2), using Neumann's method [22]. Tracing of the e^+e^-- trajectories in the PS-6 magnetic field was performed using the standard Runge–Kutta technique [23].

The simulation included the effects of multiple scattering [22] and energy loss [24] of the e^+e^--tracks inside the C_2 target.

The following Monte Carlo procedure was used. At the beginning of each simulated event, initial values were generated for each of the following:

- the energy E_γ of primary photon,
- the coordinates (x, y, z) of an interaction point in converter C_2,

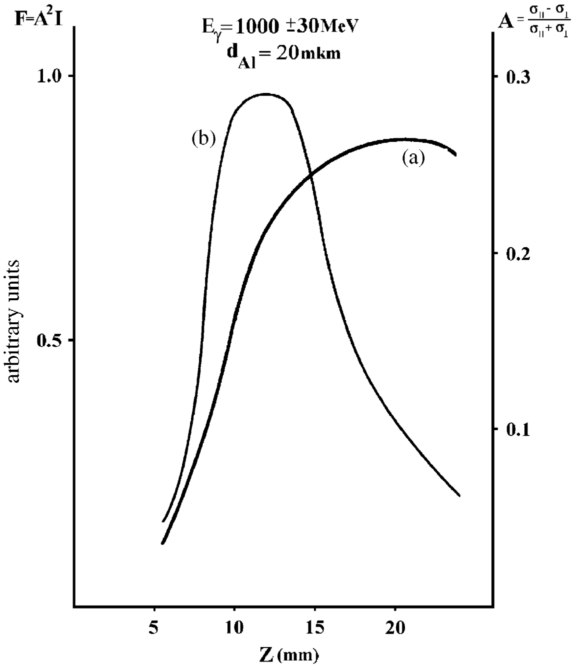

Fig. 4. Dependence of the analyzing power A (curve a) and Figure of merit F (curve b) on $Z_{\min}$, the half-height of the gap in z between the counters above the spectrometer median plane and those below it. For this study, the form factor given in Eq. (6) was used, and the energy of the peak in the CB photon spectrum was set at $E_\gamma^{\rm peak} = 1\,{\rm GeV}$.

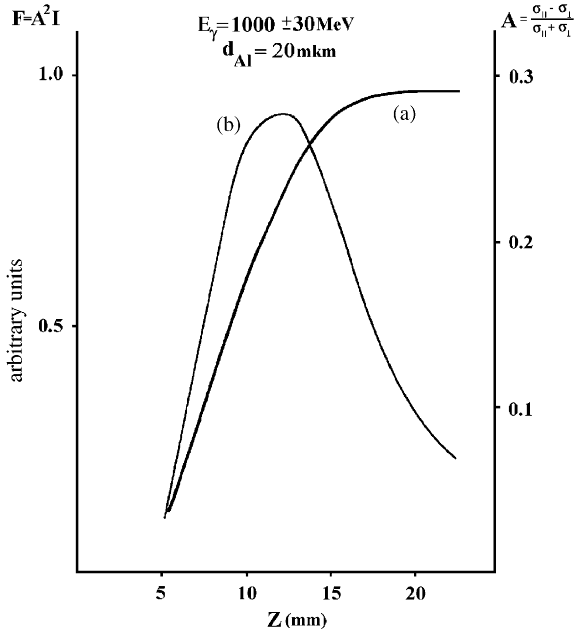

Fig. 5. Dependence of the analyzing power A (curve a) and Figure of merit F (curve b) on $Z_{\min}$, the half-height of the gap in z between the counters above the spectrometer median plane and those below it. For this study, the form factor given in Eq. (7) was used, and the energy of the peak in the CB photon spectrum was set at $E_\gamma^{\rm peak} = 1\,{\rm GeV}$.

- the electron momenta P_{e^-}, pair particles polar (θ_-, θ_+) and azimuthal (φ_-, φ_+) angles according to the differential cross section given in Eq. (2).

Starting from the initial $(P_{e^-}, P_{e^+}, \theta_-, \theta_+, \varphi_-, \varphi_+)$ values, the components of the pair $(P_{x^{+-}}, P_{y^{+-}}, P_{z^{+-}})$ momenta were calculated and corrected for multiple scattering and energy loss in the target, in order to trace them in the magnetic field of PS-6. The first goal of these studies was to find the optimal polarimeter geometry, consistent with the required energy resolution $\sigma_{E_\gamma}/E_\gamma$ and analyzing power A, as well as acceptable e^+e^- pair yields. The first variable to be studied was the vertical position $Z_{\min}$ of the innermost edge of the detector arrays, relative to the dipole median plane. This position corresponds to the lower limit of the range of polar angles θ_+ and θ_- that falls within the detector acceptance. Figs. 4 and 5 dependence of the analyzing power A (curve a) and the Figure of merit F (curve b) of $Z_{\min}$ is shown for complete screening, and for form factor CW, respectively. As can be seen in the figure, the optimum choice is $Z_{\min} = 1.2\,{\rm cm}$, which corresponds to polar angle ($\theta_{\min} = 0.4\,{\rm mrad}$) for detected particles in the momentum interval $P = 460$–$550\,{\rm MeV}/c$.

As the γ-beam energy is continuous, pairs are widely distributed both in momentum and azimuthal angles which means that the magnetic field mixes energy and direction variations between events, resulting in poor resolution in any of the kinematic quantities after magnetic analysis. As an illustration of this effect, Fig. 6(a) shows the energy distributions of symmetric e^+e^- pairs detected in the PS-6 hodoscope counters with a width of 2.5 cm over the momentum interval

$P = 460$–$550\,\mathrm{MeV}/c$. The analyzed data are fitted with Gaussian curves. As it is seen, the position distributions for mono-energetic tracks are overlapped and their separation with good resolution is not possible.

However it was found (see Fig. 6(b)), that resolution is improved by restricting the pair's range of azimuthal angles $\Delta\varphi$ using a collimator with a vertical slit. Fig. 7(a) shows the primary angular distribution of e^+e^- pairs (polar and azimutal angles) without collimation ($0.4\,\mathrm{mrad} < \theta_{e^+e^-} < 3.8\,\mathrm{mrad}$ and $\Delta\varphi = \pm 80°$). In the case of collimation (Fig. 7(b)) with a slit width of $|\Delta x| \leqslant 1\,\mathrm{cm}$, the azimuthal distribution of the pair is narrower ($\Delta\varphi = \pm 45°$) and the upper limit of polar angles is slightly reduced ($0.4\,\mathrm{mrad} < \theta_{e^+e^-} < 2.5\,\mathrm{mrad}$). As is seen from Fig. 6(b), the energy resolution of symmetric pairs is no worse than $\sigma_{E_\gamma}/E_\gamma = 1.2\%$. Thus, for symmetric pair detection using 3 hodoscope elements in the e^+ and e^- arms of the polarimeter (6 in total), a good energy resolution ($\sigma_{E_\gamma} = 12\,\mathrm{MeV}$) may be obtained in the photon energy range $E_\gamma = 900$–$1100\,\mathrm{MeV}$. Fig. 6(c) shows a section view of a collimator of width 2 cm and height 8 cm, optimized for the case of $E_\gamma^{\mathrm{peak}} = 1\,\mathrm{GeV}$ and $\Delta E_\gamma/E_\gamma = 20\%$. The inside square of dimensions with $1.4 \times 1.4\,\mathrm{cm}^2$ corresponds to γ-beam profile at the location of K_3, and the shaded areas ($0.9\,\mathrm{cm} \leqslant |Z_c| \leqslant 4\,\mathrm{cm}$) to the acceptance zone for particle tracks that have a possibility of reaching a PS-6 detector. Symmetric pairs are detected in alternate quadrants of the pair spectrometer: either left(up) with right(down) or left(down) with right(up).

The dependence of the analyzing power A in the thickness of the aluminum target C_2 is shown in Fig. 8. As shown in the figure, an increase of

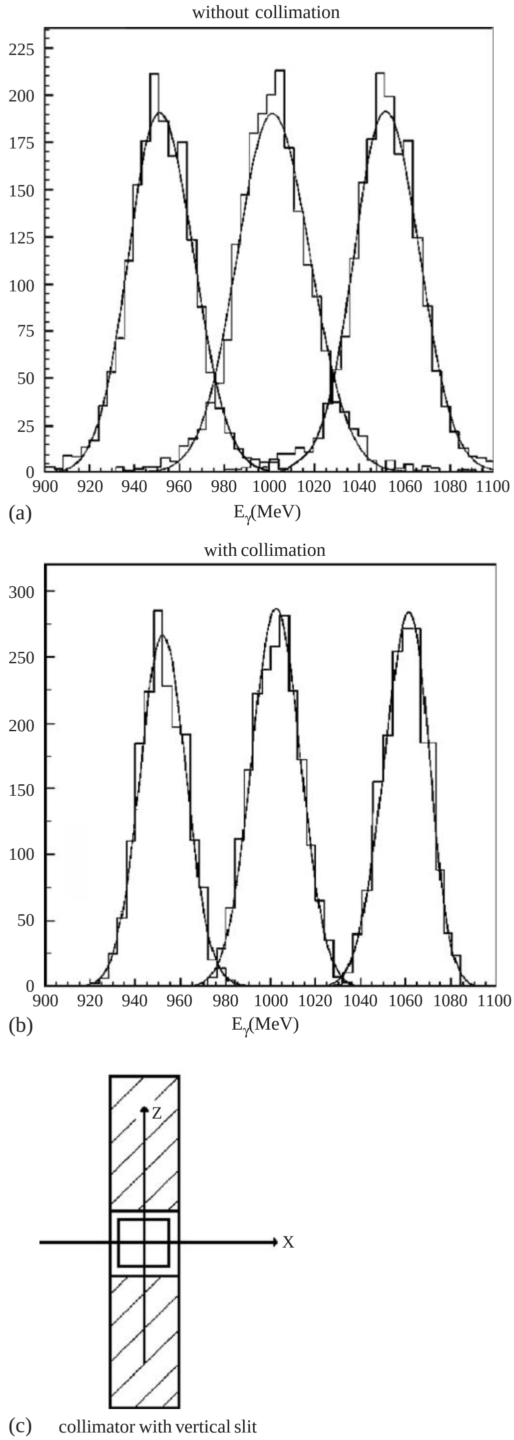

Fig. 6. Energy distributions of symmetric e^+e^- pairs detected in the hodoscopes of polarimeter PS-6, (a) without a collimator, (b) and with a collimator slit of $\Delta X = 1\,\mathrm{cm}$, for a counter width of 2.5 cm, in the track momentum interval $P = 460$–$550\,\mathrm{MeV}/c$. Panel (c) shows a sectional view of the slit collimator, showing the region of the photon beam (open box) and the acceptance regions for pair tracks (hashed regions above and below the central box).

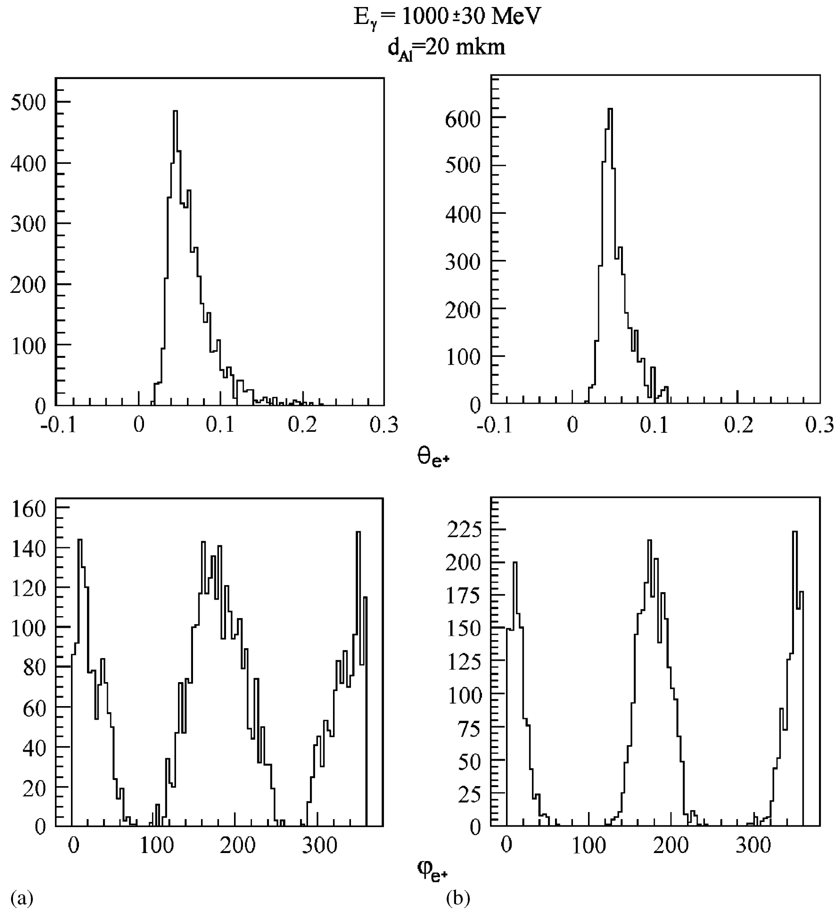

Fig. 7. Polar and azimuthal angular distributions of (e^+e^-) pairs detected in the PS-6 hodoscopes (a) without a collimator, (b) with a collimator of $\Delta X = 1\,\mathrm{cm}$.

converter's thickness from 20 to 50 μm leads to a loss of analyzing power by a factor of approximately two thirds. At a thickness of 20 μm, Monte Carlo calculations indicate a pair counting rate of a few Hz in PS-6 for a total photon beam intensity of $10^9\gamma/\mathrm{s}$.

5. Conclusion

On the basis of Monte Carlo calculations, a simple CB polarimeter for directly measuring the linear polarization a photon beam in the energy range around 1 GeV an accuracy of 0.02 has been developed by the method of incoherent pair production on an amorphous target. It is shown that using hodoscopes of scintillating counters vertically shifted from the polarimeter median plane and a collimator with a vertical slit leads to a polarimeter with an analyzing power of 0.25 with expected yields of useful events on the level of a few Hz.

Measurements of the beam polarization at the Yerevan synchrotron CB photon source will provide an important check of the reliability of indirect polarimetry methods, and provide a direct measurement of the atomic form factor that is relevant to coherent bremsstrahlung.

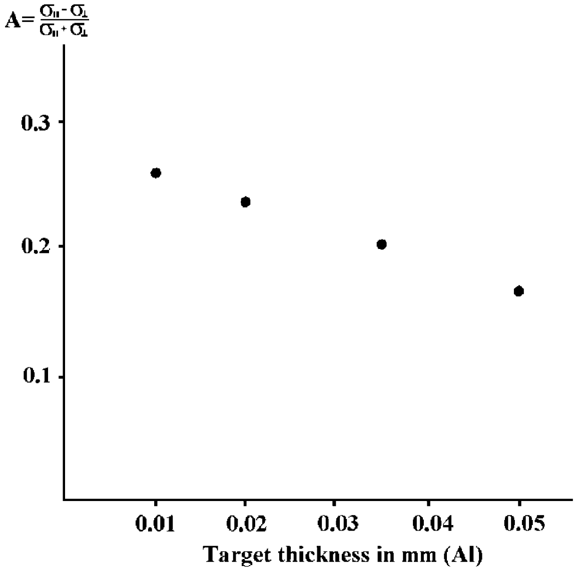

Fig. 8. The dependence of the analyzing power (A) on the converter (C_2) thickness in the case an aluminum target.

Acknowledgements

Authors express their gratitude to R. Avagyan, A. Aganyants, S. Darbinyan, K. Dallakyan and S. Taroyan for useful discussions.

The work is supported by CRDF Grant (CRDF AP2-2305-YE-02).

References

[1] H. Uberall, Phys. Rev. 103 (1956) 1055.
[2] H. Uberall, Phys. Rev. 107 (1957) 233.
[3] G. Diambrini-Palazzi, Rev. Mod. Phys. 40 (1968) 611.
[4] G. Bologna, et al., IL Nuovo Cimento XLII A N4 (1966) 844.
[5] U. Timm, Fortschr. Phys. 17 (1969) 765.
[6] D. Lohmann, et al., Nucl. Instr. and Meth. A 343 (1994) 494.
[7] C.N. Yang, Phys. Rev. 77 (1950) 722.
[8] J.H. Berlin, L. Madansky, Phys. Rev. 78 (1950) 623.
[9] L.C. Maximon, H. Olsen, Phys. Rev. 126 (1962) 310; H. Olsen, L.C. Maximon, Phys. Rev. 114 (1959) 887.
[10] G. Barbiellini, et al., Phys. Rev. Lett. 9 (1962) 396.
[11] L.C. Maximon, H.A. Gimm, Phys. Rev. A 23 N1 (1981) 172; V.F. Boldyshev, et al., Phys. Part. Nucl. 25 (1994) 292.
[12] M. Kobayashi, K. Kondo, Nucl. Instr. and Meth. 104 (1972) 101.
[13] B. Wojtsekhowski, et al., CLAS-NOTE 98-018, 1998.
[14] R. Avagyan, et al., hep-ex/9908048 2 (1999).
[15] D.T. Cromer, J.T. Waber, Acta Cryst. A 18 (1968) 104.
[16] R. Avakyan, et al., Izvestia Acad. Nauk Arm. SSR, Physics 10 (1975) 61.
[17] H. Hakobyan, et al., YERPHI-908(59)-86 (1986).
[18] H. Hakobyan, G. Karapetyan, YERPHI-1138(15)-89 (1989).
[19] S. Darbinyan, et al., YERPHI - 1589(10) (2003).
[20] A. Avetisyan, et al., YERPHI-1325(20)-91 (1991).
[21] G. Bologna, Nuovo Cimento 49 A (1967) 756 W. Kaune, et al., Phys. Rev. D 11, N3, 478 (1975).
[22] Particle Data Group, Phys. Rev. D 45 (1992).
[23] A. Sirunyan, et al., YERPHI-491(34)-81 (1981).
[24] B. Star, et al., Springer Tracts in Modern Physics, vol. 124, 1993.